TECHNICAL MEMORANDUM

302

The comparative impact of the assimilation of SSM/I and TMI brightness temperatures in the ECMWF 4D-Var system

V. Marécal, E. Gérard,
J-F. Mahfouf and P. Bauer

Research Department

May 2000

European Centre for Medium-Range Weather Forecasts
Europäisches Zentrum für mittelfristige Wettervorhersage
Centre européen pour les prévisions météorologiques à moyen

Abstract

This paper studies the impact of assimilating TMI (Tropical Rainfall Measuring Mission Microwave Imager) brightness temperatures in the ECMWF (European Centre for Medium-Range Weather Forecasts) four-dimensional variational assimilation system (4D-Var). The methodology is similar to the one developed operationally for SSM/I (Special Sensor Microwave/Imager) radiometers. First, a one-dimensional variational (1D-Var) approach is used to retrieve specific humidity profiles, sea surface wind speed and cloud liquid water path. Then, the first two quantities are assimilated in the 4D-Var analysis system. Results show an improvement of 1D-Var product accuracy when using TMI instead of SSM/I brightness temperatures. This is related to the characteristics of the TMI radiometer which allow a better estimate of surface parameters and of water vapour in tropical conditions. Consequently, 4D-Var analyses of TCWV are improved using TMI data. The experiment with TMI observations give a smaller increase in global humidity than the experiment with SSM/I data. This leads with TMI data to a reduction of the model precipitation spin-down at the beginning of the forecasts. The impact on the low level wind analysis is small with either SSM/I or TMI data. Forecast performance with TMI is genrally improved compared to a control experiment without any SSM/I and TMI data. TMI experiment scores are better than those obtained for SSM/I experiment for the geopotential at 1000 hPa in the Northern hemisphere and for the tropical winds at 200 hPa.

1 Introduction

One major source of improvement for global atmospheric analyses and forecasts comes from the use of more accurate observations in operational data assimilation systems. Over oceans, conventional observations are scarce and spaceborne microwave data provide a valuable piece of information on surface and atmospheric parameters. In particular, the Defense Meteorological Satellite Program (DMSP) Special Sensor Microwave Imager (SSM/I) (Hollinger *et al.* 1990) has been used in numerous studies to retrieve total column water vapour (e.g. Alishouse *et al.* 1990, Bauer and Schluessel 1993), cloud liquid water path (e.g. Karstens *et al.* 1994, Gérard and Eymard 1998), sea surface wind (e.g. Goodberlet *et al.* 1990), rainfall (e.g. Kummerow *et al.* 1996), snow cover and sea ice (e.g. Ferraro *et al.*, 1996). Most of these algorithms use a regression approach which is easy to implement but generally allows the retrieval of only one geophysical parameter at a time.

At ECMWF (European Centre for Medium-Range Weather Forecasts), a one dimensional variational (1D-Var) method was developed for retrieving simultaneously the specific humidity profile, the sea surface wind speed (SSWS) and the cloud liquid water path (LWP) from SSM/I brightness temperatures over oceans in non-rainy areas (Phalippou 1996). These parameters are calculated following the theory of non-linear optimal estimation (Rodgers 1976) and are therefore the best set of parameters that explains the observed brightness temperatures while being consistent with the available *a priori* information provided by a short-term model forecast. Total column water vapour (TCWV) and SSWS retrievals from the 1D-Var have been assimilated operationally in the ECMWF four-dimensional variational (4D-Var) analysis system since June 1998 and October 1999, respectively. Gérard and Saunders (1999) showed that the impact of the 1D-Var TCWV assimilation on forecast scores is positive or neutral depending on the season and on the region.

Meanwhile, the Tropical Rainfall Measuring Mission (TRMM) was launched in November 1997. The main objective of this observation satellite is to measure rainfall and energy exchanges of tropical and subtropical regions (Simpson *et al.* 1996). On board, three complementary instruments measure precipitation (Kummerow *et al.* 1998) in particular a microwave radiometer named TMI (TRMM Microwave Imager). The TMI radiometer is identical to SSM/I except for two aspects. Firstly, TMI includes two additional channels: 10.65 GHz vertical polarization and 10.65 GHz horizontal polarization. Secondly, the frequency of the channel most sensitive to water vapour (around 22 GHz) is slightly shifted compared to SSM/I. Both differences can be of importance for the retrieval of surface and atmospheric parameters, in particular for TCWV, SSWS and LWP. In this paper we study the impact on analyses and forecasts of using TMI brightness temperatures instead of SSM/I ones in the ECMWF 4D-Var assimilation system.

A brief description of the TMI and the SSM/I characteristics is provided in section 2. Section 3 gives a summary of the 1D-Var retrieval method. In this section results are shown on the theoretical accuracy of the 1D-Var products obtained using TMI and SSM/I brightness temperatures. The assimilation of 1D-Var TCWV and SSWS in the 4D-Var system is described

in section 4. Analysis and forecast results are discussed in sections 5 and 6, respectively. Concluding remarks are given in section 7.

2 Characterictics of SSM/I and TMI instruments

The SSM/I radiometers (Hollinger *et al.* 1990) fly on board DMSP satellites which are in a polar orbit at an altitude of about 830 km. The SSM/I is a seven-channel radiometer whose frequencies are 19.35, 22.235, 37.0 and 85.5 GHz. All frequencies are received in vertical (V) and horizontal (H) polarizations except for the 22.235 GHz which is only received in vertical polarization.

The TMI radiometer (Kummerow *et al.* 1998) is on board the TRMM satellite which is in a circular orbit at an altitude of about 350 km with a 35^o inclination angle resulting in a coverage of the tropical and sub-tropical areas only (between -40° to +40° latitude approximately). The TMI is a nine-channel radiometer based upon the SSM/I. The key differences with SSM/I are two additional channels at 10.65 GHz with H and V polarizations and a water vapour channel at 21.3 GHz vertical polarization instead of 22.235 GHz vertical polarization. This shift off the centre of the water vapour line reduces saturation effects in tropical regions.

SSM/I and TMI have both a conical scan geometry corresponding to a median zenith angle (i.e. viewing angle at the earth's surface) of 53.1^o and 52.8^o, respectively. Because of the earth's oblateness and the eccentricity of the satellite orbit, this angle varies with latitude. For SSM/I this effect is small because of its orbit altitude. For TMI which flies in a lower orbit, the variation of the zenith angle ranges between about 47^o and 53^o. The SSM/I swath (1400 km) is much broader than the TMI swath (758.5 km). Tables 1 and 2 give the effective field of view (EFOV) of the half-power beam widths together with the radiometric sensitivities (noise equivalent in brightness temperature or NeΔT) for SSM/I and TMI, respectively. SSM/I EFOVs are about twice as coarse as TMI EFOVs and TMI has a better radiometric accuracy compared to SSM/I.

The SSM/I data used in this study are from the DMSP-F13 satellite only. The TMI brightness temperatures are the 1B11 NASA/NASDA product level 4. This product is corrected for a known calibration error following Wentz (1999, personal communication).

Frequency (GHz)	19.35	22.235	37.0	85.5
Polarization	V&H	V	V&H	V&H
EFOV (km)	63x43	60x40	37x28	15x13
NeΔT (K)	0.8	0.8	0.6	1.1

Table 1: *SSM/I spatial resolution (EFOV) and radiometric accuracy (NeΔT).*

Frequency (GHz)	10.65	19.35	21.3	37.0	85.5
Polarization	V&H	V&H	V	V&H	V&H
EFOV (km)	63x37	30x18	23x18	16x9	7x5
NeΔT (K)	0.63V/0.54H	0.50V/0.47H	0.71V	0.36V/0.31H	0.52V/0.93H

Table 2: *TMI spatial resolution (EFOV) and radiometric accuracy (NeΔT).*

3 1D-Var retrieval

3.1 Method

Only a brief summary of 1D-Var method is given in this sub-section. A detailed description can be found in Phalippou (1996) with updates in Gérard and Saunders (1999). We define $\mathbf{x}$ as the control variable which is a 17 element vector containing the natural logarithm of the specific humidity on 15 fixed pressure levels between 300 hPa and 1000 hPa, the sea surface wind speed and the cloud liquid water path. We seek the best estimate of $\mathbf{x}$ knowing an *a priori* or background vector $\mathbf{x^b}$ given by the ECMWF first-guess (short-term forecast) and a coincident observation vector $\mathbf{y^o}$. If the background and observation errors are uncorrelated and each has a Gaussian distribution, the maximum likelihood estimator of the state vector $\mathbf{x}$ is the minimum of the following cost-function:

$$J(\mathbf{x}) = \frac{1}{2}[\mathbf{x} - \mathbf{x^b}]^{\mathrm{T}}\mathbf{B}^{-1}[\mathbf{x} - \mathbf{x^b}] + \frac{1}{2}[\mathbf{y^o} - H(\mathbf{x})]^{\mathrm{T}}\mathbf{R}^{-1}[\mathbf{y^o} - H(\mathbf{x})] \quad (1)$$

where $H(\mathbf{x})$ is the observation operator, $\mathbf{R}$ the observation error covariance matrix and $\mathbf{B}$ the background error covariance matrix.

The operator H is the radiative transfer model which computes brightness temperatures from the control vector $\mathbf{x}$. The fast radiative transfer model used in 1D-Var (Phalippou 1996) takes into account the absorption by atmospheric gases and by cloud water and includes a fairly detailed description of sea-surface interactions with radiation. However, scattering by rain and ice particles is not included leading to erroneous results in rainy areas. To allow the assimilation of TMI brightness temperatures in 1D-Var, the fast radiative transfer model was updated to include the two additional TMI channels and the modification of the water vapour channel frequency. Because in the 1D-Var each observation consists of a set of brightness temperatures, retrieved products are mean values over the area observed by the microwave radiometer (i.e. the EFOV). Thus 1D-Var TCWV and SSWS from TMI data are representative of a smaller spatial area than both SSM/I products and ECMWF model grid boxes.

The variation of the zenith angle for TMI is not taken into account in the fast radiative transfer model because it would lead to an important increase in computing time and memory storage which is hardly affordable in the context of 4D-Var assimilation of 1D-Var products. Instead, a constant value taken equal to the most frequent TMI zenith angle (52.8^o) is used. More than

85% of the measurements correspond to an angle between 52.6° and 52.9°, as illustrated in Fig. 1a showing the accumulated frequency distribution of the zenith angle for 12 arbitrary orbits corresponding to a total sample size of 430,000 cases.

The constant zenith angle assumption used in the fast radiative tranfer model requires attention because surface reflection and emission have strong variations with the zenith angle. For an estimation of the bias induced by this hypothesis, a simulation was carried out using the distribution of zenith angles along TRMM overpaths given in Fig. 1a. A set of atmospheric profiles of pressure, temperature, and humidity from radiosondes was taken which included measurements of windspeed near the ocean surface. For each profile, brightness temperatures were calculated for various zenith angles following the frequency distribution obtained from TMI data giving a sample size of 26,150 cases. For each frequency and polarization measured by the TMI, the overall bias and standard deviation (RMSE) between profiles with varying angles and those with a fixed angle of 52.8° were computed. Thus the net angle effect including variations in surface roughness and atmospheric opacity are retrieved. Fig. 1b and 1c show the results. Since vertically polarized emissivity varies strongly with angle and is less sensitive to windspeed, biases between 0.45 K and 0.25 K with RMSE's between 1.65 K and 0.95 K are obtained at 19.35 and 85.5 GHz, respectively. For horizontally polarized emissivities, the stronger impact of windspeed and atmospheric transmission results in rather small biases below 0.2 K and RMSE's below 0.75 K.

In Equation (1), the observation covariance matrix $\mathbf{R}$ takes into account both observation and forward model errors in terms of brightness temperatures. They are assumed to be uncorrelated, i.e. the $\mathbf{R}$ matrix is diagonal and the square root of its diagonal elements is set to an approximate value of the NeΔTs of the instruments (see Tables 1 and 2) plus assumed errors in the radiative transfer model. For SSM/I, a value of 2 K is used for all channels except at 85.5 GHz where the errors are set to 3 K in order to take into account the higher NeΔTs. For TMI, the errors are set to 2 K for all the channels. This value accounts for the bias induced by the constant zenith angle assumption (lower than 0.5 K) and for the NeΔTs which are smaller than SSM/I ones.

The background error covariance matrix for specific humidity is the one used in the operational SSM/I 1D-Var. Values are given in Gérard and Saunders (1999). A 2 $m.s^{-1}$ first guess SSWS error is assumed following the results of a comparison between the ECMWF first guess wind field and ERS-1 scatterometer measurements (Stoffelen and Anderson 1994). The cloud liquid water path background error is set to 0.2 $kg.m^{-2}$ which represents a weak constraint allowing the observations to largely influence the retrieved cloud LWP. This choice is explained in Gérard and Saunders (1999).

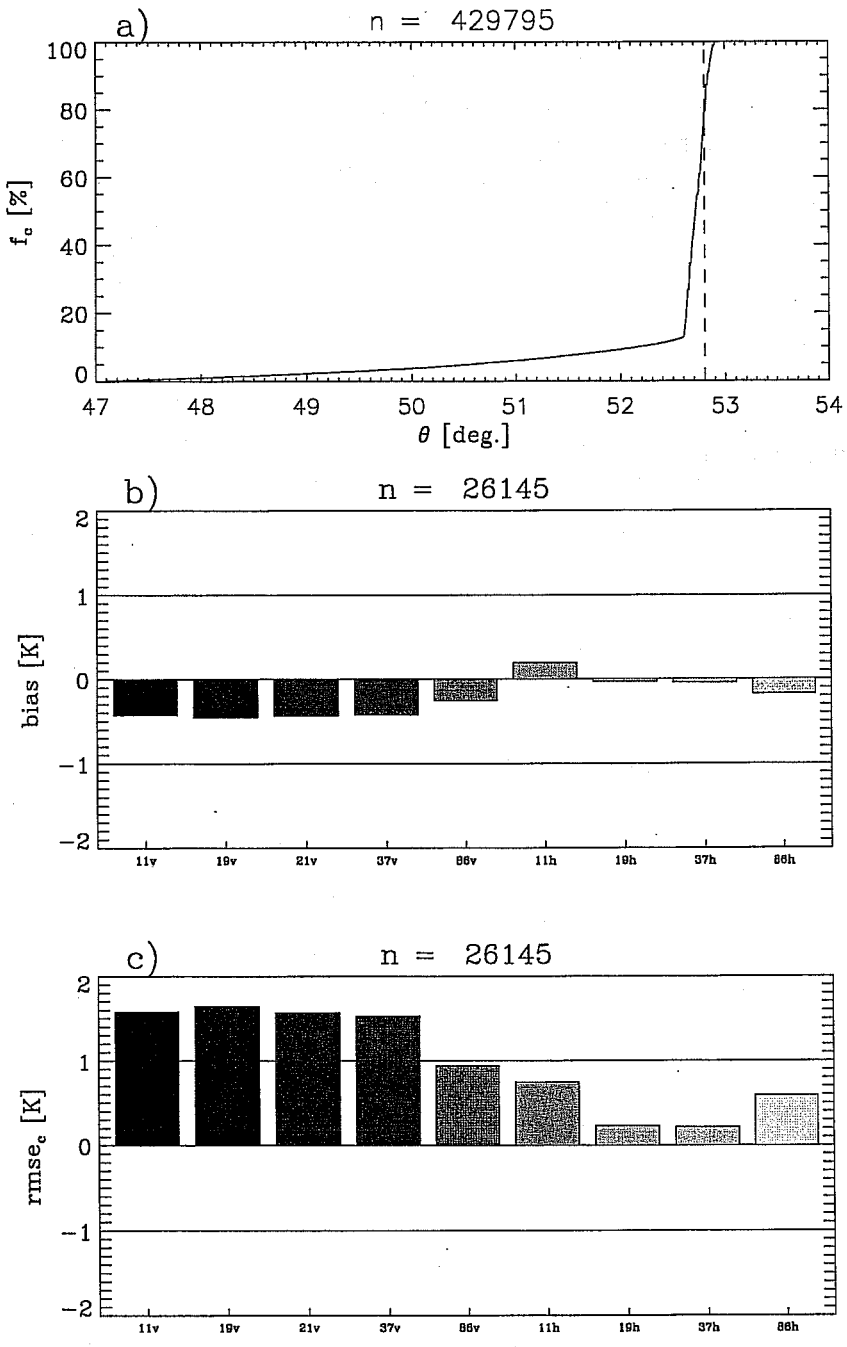

Figure 1: *Accumulated frequency distribution of TMI zenith angles from 12 orbits (a). The dashed lines indicate nominal zenith angle of 52.8°. Brightness temperature bias simulation using above distribution when constant zenith angle is assumed (b); same for standard deviation (c).*

Frequency (GHz) and polarization	19V	19H	22V	37V	37H	85V	85H
Mean bias (K)	-1.66	-1.71	-0.34	0.06	-2.05	1.56	1.15

Table 3: *Mean bias correction for SSM/I (to be added to the observed brightness temperatures) computed using a procedure based on Alishouse et al. (1990)'s algorithm.*

Frequency (GHz) and polarization	10V	10H	19V	19H	22V	37V	37H	85V	85H
Mean bias (K)	-1.33	-0.82	0.20	-0.72	0.26	0.59	-0.95	1.54	1.93

Table 4: *Mean bias correction for TMI (to be added to the observed brightness temperatures) computed using a procedure based on model first-guess humidity.*

3.2 Bias correction

Any bias in the observed brightness temperatures or in the radiative transfer model used in 1D-Var can lead to biased retrievals. Thus, a brightness temperature bias correction is applied to take into account these two possible biases. For SSM/I, the operational procedure is based on the global comparison of the TCWV estimates provided by the 1D-Var and by a regression algorithm applied to SSM/I brightness temperatures (Alishouse *et al.* 1990). The bias correction values for SSM/I were recomputed with the latest model configuration. They are given in Table 3 since they differ from Gérard and Saunders (1999).

Since TMI and SSM/I water vapour channels are slightly different, it is not possible to use Alishouse *et al.* (1990)'s algorithm to compute the TMI brightness temperature bias correction. Moreover, no validated regression algorithm for TCWV estimation is yet available for TMI frequencies. Thus, the bias correction for this radiometer was obtained using TCWV estimates from the model first-guess. This procedure, which is also used for ATOVS radiances at ECMWF, assumes that the first-guess humidity is unbiased. Bias corrections for TMI are given in Table 4. They are all smaller than 2 K and of the same order of magnitude as SSM/I bias corrections.

To evaluate the influence of using different procedures for the bias correction, the latter was recomputed for SSM/I using the model first-guess humidity instead of Alishouse *et al.* (1990)'s estimate of TCWV. Results are given in Table 5. Bias correction found for SSM/I using the two procedures is very similar (Tables 3 and 5). The differences obtained are within the range of bias correction variations that can be found when running the "Alishouse" bias correction procedure for different seasons or with different versions of the model. Consequently, there is no significant difference between the two bias correction procedures.

Frequency (GHz) and polarization	19V	19H	22V	37V	37H	85V	85H
Mean bias (K)	-1.71	-1.90	-0.34	0.01	-2.11	1.83	0.89

Table 5: *Mean bias correction for SSM/I (to be added to the observed brightness temperatures) computed using a procedure based on model first-guess humidity.*

3.3 Methodology for 1D-Var theoretical accuracy estimation

A by-product of the 1D-Var method is the estimation of the standard deviation of the *a posteriori error* or "theoretical accuracy" of the retrieved products. It can be shown (Rodgers 1976) that the *a posteriori* error covariance matrix $\mathbf{A}$ of the estimation $\mathbf{x}$ can be approximated by:

$$\mathbf{A} = (\mathbf{B}^{-1} + \mathbf{H}^{\mathrm{T}}\mathbf{R}^{-1}\mathbf{H})^{-1} \quad (2)$$

$\mathbf{H}$ is the tangent linear observation operator obtained from the radiative transfer model (i.e. its elements are the partial derivatives of the simulated brightness temperatures with respect to the control variable $\mathbf{x}$). The *a posteriori* error variances of the estimate of $\mathbf{x}$ are given by the diagonal elements of $\mathbf{A}$. In order to assess how much the observations improve the *a priori* knowledge, $\mathbf{A}$ must be compared to $\mathbf{B}$. The improvement factor is defined as the ratio of the *a priori* to the *a posteriori* error standard deviations of each product. It is greater than or equal to 1. An improvement factor of 1 means that the *a priori* knowledge of this product has not been improved by the satellite measurements. The larger the ratio is, the better the improvement on the *a priori* knowledge of $\mathbf{x}$ is. This variational framework was used by Phalippou and Gérard (1996) to infer the theoretical accuracies of the SSM/I 1D-Var products.

3.4 Results on accuracy assessment

The *a posteriori* errors were computed from a large number of atmospheric and surface conditions for SSM/I and TMI. Fig. 2 shows the improvement factor for TCWV and SSWS as a function of TCWV, and of SSWS, respectively.

The improvement factors for TCWV computed from SSM/I characteristics range from 2 to 10 for values of TCWV from 5 to 70 kg.m^{-2}. The theoretical accuracy for TMI is better than for SSM/I; the improvement factor ranges from 2 to 13. The addition of the pair of low frequency channels in the TMI instrument provides a better retrieval of surface parameters and consequently of atmospheric humidity. The fact that TCWV accuracy is improved more significantly for high water vapour values suggests that the saturation of the brightness temperatures with TCWV is less important for the TMI water vapour absorption frequency than that of SSM/I.

The improvement factors for SSWS retrieved with SSM/I and TMI are larger in strong wind conditions. However, above 15 m.s^{-1}, it is suspected that the large improvement factor found

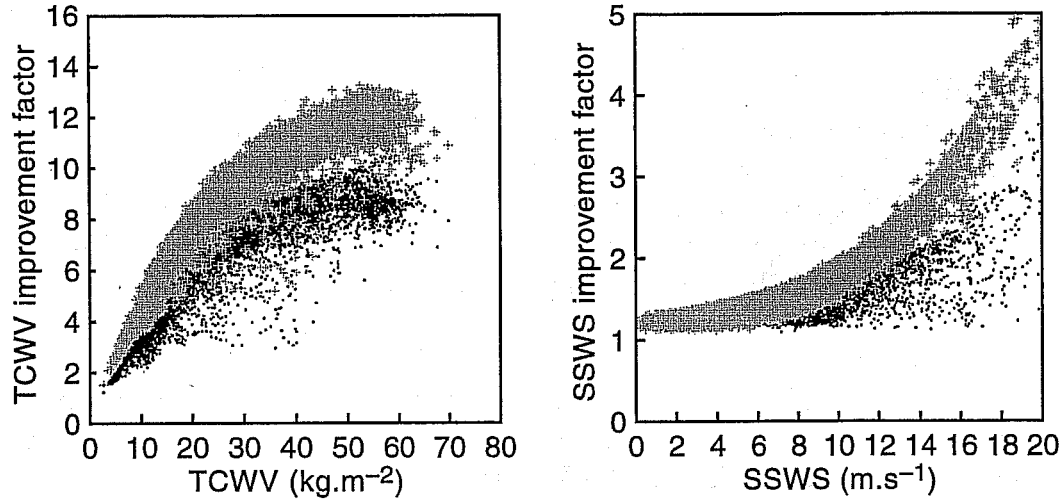

Figure 2: *TCWV improvement factor as a function of TCWV values (left panel) and SSWS improvement factor as a function of SSWS values (right panel). Black dots are for SSM/I and grey crosses for TMI*

for both SSM/I and TMI is due to an unrealistic modelling of the sea surface for high wind speeds, which leads to an underestimation of the wind speed error. Fig. 2 shows that TMI data provides a better improvement factor for SSWS that is related to the use of the 10 GHz frequency in the 1D-Var computation for TMI. It should be noted that in the calculation of the improvement factor (Equation (2)), the TMI zenith angle has a constant value as in the 1D-Var minimization. Consequently, the accuracy results do not take into account the impact of this simplification which slightly deteriorates TMI SSWS theoretical accuracy.

4 4D-Var assimilation experiments

4.1 Method

The operational ECMWF assimilation system is based on an incremental four-dimensional variational method (Rabier *et al.* 2000, Mahfouf and Rabier 2000, Klinker *et al.* 2000). 4D-Var seeks an optimal balance between observations and the dynamics of the atmosphere by finding a model solution which is as close as possible, in a least-square sense, to the background information (model short-term forecast) and to the observations available over a given time period (currently six hours). The incremental formulation of 4D-Var (Courtier *et al.* 1994) consists of computing the background trajectory and the departures (observations minus model) using the full non-linear model at high resolution including a full set of physical parameterizations, and minimizing the cost-function in a low resolution space for the increments at initial time

using a tangent linear model and its adjoint with a limited set of physical parameterizations (Mahfouf 1999).

The assimilation in 4D-Var of 1D-Var TCWV from SSM/I measurements over ocean was implemented operationally in June 1998. It has proved to be beneficial for the analyses and forecasts (Gérard and Saunders 1999). A detailed description of the procedure used for SSM/I TCWV assimilation is given in Gérard and Saunders (1999). The errors on SSM/I TCWV estimates used operationally in 4D-Var are derived from an empirical formulation assuming a linear variation of the TCWV error with TCWV values. This formulation is also used to determine TMI TCWV errors.

The assimilation of 1D-Var SSWS from SSM/I has been done operationally since October 1999. Results show neutral or positive impact on the analyses and forecasts (Gérard and McNally 1999). The errors on SSM/I SSWS used in 4D-Var were modelled as a function of the wind speed by a quadratic formulation. This formulation is also used for TMI SSWS errors.

The thinning procedures applied to SSM/I brightness temperatures and to SSM/I 1D-Var TCWV are detailed in Gérard and Saunders (1999). They are performed to reduce correlations between observations in 4D-Var. Similar procedures are used for TMI : the observations are sampled at a 125 km resolution in 1D-Var and TCWV retrievals are thinned at 250 km resolution for use in 4D-Var. Operationally, a quality control is performed to SSM/I 1D-Var retrievals before entering the 4D-Var system. The 1D-Var minimization has to be successful and the brightness temperatures recomputed from 1D-Var products have to be close to SSM/I observations. The same quality control is applied to TMI 1D-Var products. This procedure is completed by a rejection of SSM/I and TMI 1D-Var retrievals in rainy areas. Rainy profiles are diagnosed by applying a regression algorithm to the observed radiances from Bauer and Schluessel (1993) for SSM/I and Bauer (1999, personal communication) for TMI.

4.2 Design of the experiments

Three assimilation experiments were conducted to assess the impact of using TMI instead of SSM/I brightness temperatures in the ECMWF 4D-Var system. The model configuration used (Cycle 21R4) is $T_L319L60$ (triangular truncation at total wave number 319 and 60 levels). It corresponds approximately to a 60 km resolution. The 60 vertical levels are spread between the surface and the 0.1 hPa altitude. The experiments were run for the period 7 to 21 September 1999. The humidity data used in these experiments are detailed in Table 6. The first experiment does not make use of any SSM/I or TMI products in 4D-Var (Control). The second experiment is identical to the Control experiment except that it includes the assimilation of SSM/I TCWV and SSWS as in the operational configuration (SSM/I experiment). In the last experiment, TMI TCWV and SSWS are assimilated while no SSM/I 1D-Var products are used (TMI experiment). A series of 10-day forecasts were run from the 12 UTC analyses.

Type of observation	Control	SSM/I	TMI
Specific humidity profiles below 300 hPa (TEMP)	Yes	Yes	Yes
Surface relative humidity (SYNOP)	Yes	Yes	Yes
TCWV in non-rainy areas over oceans (SSM/I)	No	Yes	No
TCWV in non-rainy areas over oceans (TMI)	No	No	Yes

Table 6: *Humidity data used in the 4D-Var assimilation for Control, SSM/I and TMI experiments*

Since TRMM only covers the tropics and the subtropics, results (tables and figures) of these three experiments are given and discussed for the latitude band sampled by TMI. The term "global" represents hereafter this latitude band, except in subsection 6b where the full globe is considered.

5 Impact on analyses

5.1 Statistics of model departures from observations

The global mean statistics of the 4D-Var assimilation of 1D-Var TCWV and SSWS are shown in Fig. 3 and 4. The background departure is the difference between the observation and the background (short-term forecast). The analysis departure is the difference between the observation and the analysis. Here the observations are the 1D-Var SSWS and TCWV. To compute these statistics, the background and analysis fields are converted into TCWV or SSWS and interpolated at the observation location. Note that in Fig. 3 and 4 the number of "1D-Var TCWV" observations used in 4D-Var is larger by roughly 50% for the TMI experiment than for the SSM/I one. This is related to the different spatial coverage between TMI and SSM/I. A non negligible number of SSM/I observations are collected at mid and high latitudes and are not taken into account in the statistics presented.

Fig. 3 shows that the mean value of the TCWV background departures is positive for both TMI and SSM/I experiments. Thus both SSM/I and TMI diagnose on average a moister atmosphere than the model. Nevertheless, for TMI this bias is noticeably smaller than for SSM/I leading to a RMS (root mean square) for background departures slightly smaller for TMI than for SSM/I. The mean and RMS of the analysis departures are smaller with TMI observations showing a better fit to observations. For both experiments, the mean and RMS of the analysis departures are smaller by a factor 2 and 1.5 respectively than the corresponding background departures. This indicates that an significant part of the information from SSM/I TCWV and TMI TCWV has been extracted by the 4D-Var system.

Fig. 4 shows the global mean statistics of the 4D-Var assimilation of 1D-Var SSWS. More

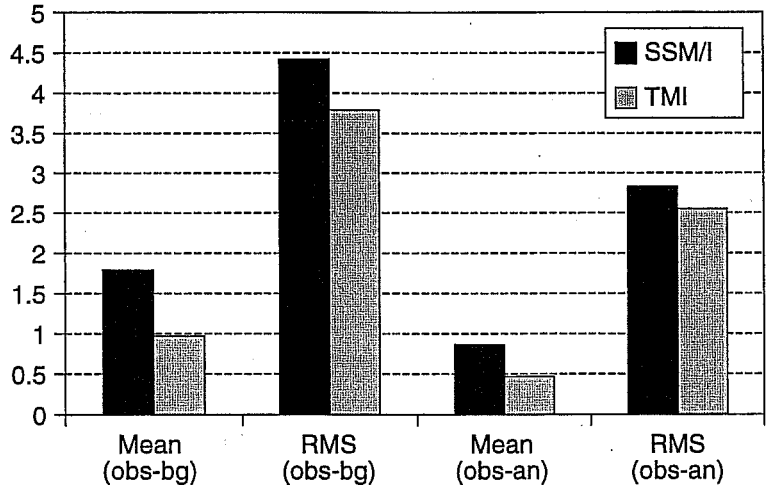

Figure 3: *Global mean statistics of the 1D-Var TCWV used in 4D-Var for the two-week period. Units are in kg* m^{-2}. *The background departure is the "1D-Var TCWV observation" minus the background fields (short term forecast) converted into TCWV and interpolated at the observation location. The analysis departure is "1D-Var TCWV observation" minus 4D-Var analysed fields converted into TCWV and interpolated at the observation location. The number of observations used to compute the statistics is 50952 for SSM/I and 79144 for TMI.*

"SSWS observations" than "TCWV observations" are used in each experiment because the thinning procedure is done at 125 km resolution for SSWS and at 250 km for TCWV. Both SSM/I and TMI experiments show a reduction of the RMS of the analysis departures compared to the RMS of the background departures which shows that 1D-Var SSWS information have been efficiently assimilated in the 4D-Var. SSM/I observations lead to smaller mean and RMS values of background and analysis departures than TMI observations. In particular, background departures are unbiased with SSM/I while TMI exhibits a 0.230 m s^{-1} bias. This means that TMI SSWSs tend to be larger than the model winds. This can be explained by two main reasons. Firstly, the effect of the variation of the zenith angle for TMI was not taken into account in the 1D-Var radiative transfer model. The expected consequence of this simplification is a small but non-negligible error in the 1D-Var SSWS retrievals from TMI observations. Secondly, TMI EFOVs are smaller than the model resolution for all channels even for low frequencies. This means that 1D-Var SSWS estimates from TMI brightness temperatures are representative of a smaller scale than the model wind field. This representativeness problem affects less SSM/I SSWS estimation because of the size of the EFOVs is closer to the model resolution.

For the above reasons, one cannot expect a large improvement of the 4D-Var low level wind analysis when using TMI brightness temperatures. This representativeness problem is less important for TCWV because water vapour has larger horizontal correlation scales than sea surface wind and can be considered homogeneous at the model grid scale. Moreover, since the analysis of TCWV in 4D-Var is weakly coupled to the analysis of SSWS, an independent interpretation of the results on TCWV and SSWS is possible. It was checked in a one-day

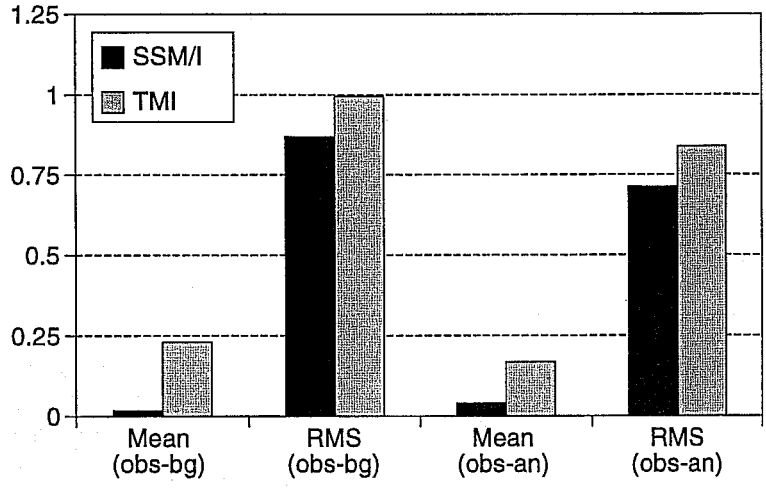

Figure 4: *Same as Figure 3 but for 1D-Var SSWS. Units are in m s^{-1}. The number of observations used to computed the statistics is 164535 for SSM/I and 225589 for TMI*

assimilation experiment that the TCWV results are not modified when no TMI or SSM/I SSWSs are assimilated in 4D-Var.

5.2 Analysis of total column water vapour

Fig. 5 shows the mean TCWV field from the 4D-Var analyses averaged over the 2-week period for the three experiments. SSM/I and TMI experiments provide very similar TCWV fields. Compared to the Control experiment, they give generally higher TCWV values in most areas. This shows, in agreement with results from Fig. 3, that SSM/I and TMI 1D-Var tend to estimate a moister atmospheric state compared to the model short-term forecast and that the 4D-Var analysis retains part of this humidity. To compare more precisely TCWV analysed fields from the SSM/I and TMI experiments, maps of differences with respect to the Control experiment are displayed in Fig. 6. Both SSM/I and TMI experiments tend to increase humidity in most places compared to the Control experiment. Moreover, there is a good consistency between the TMI and SSM/I fields. Nevertheless, TMI assimilation tends to increase less the global mean TCWV (34.78 kg m^{-2}) than the SSM/I assimilation (35.10 kg m^{-2}) compared to the Control experiment (33.66 kg m^{-2}).

To evaluate the quality of TMI experiment analyses the RMS of TCWV increments is calculated. These increments are the departure in TCWV between the background and the analysis. In regions where no humidity data are assimilated, RMS values are very small because the analysis is not modified and remains close to the background humidity field. In regions where humidity observations are assimilated, a reduction of the RMS means that short-range forecasts are closer to the observations and that smaller corrections are necessary during the assimilation.

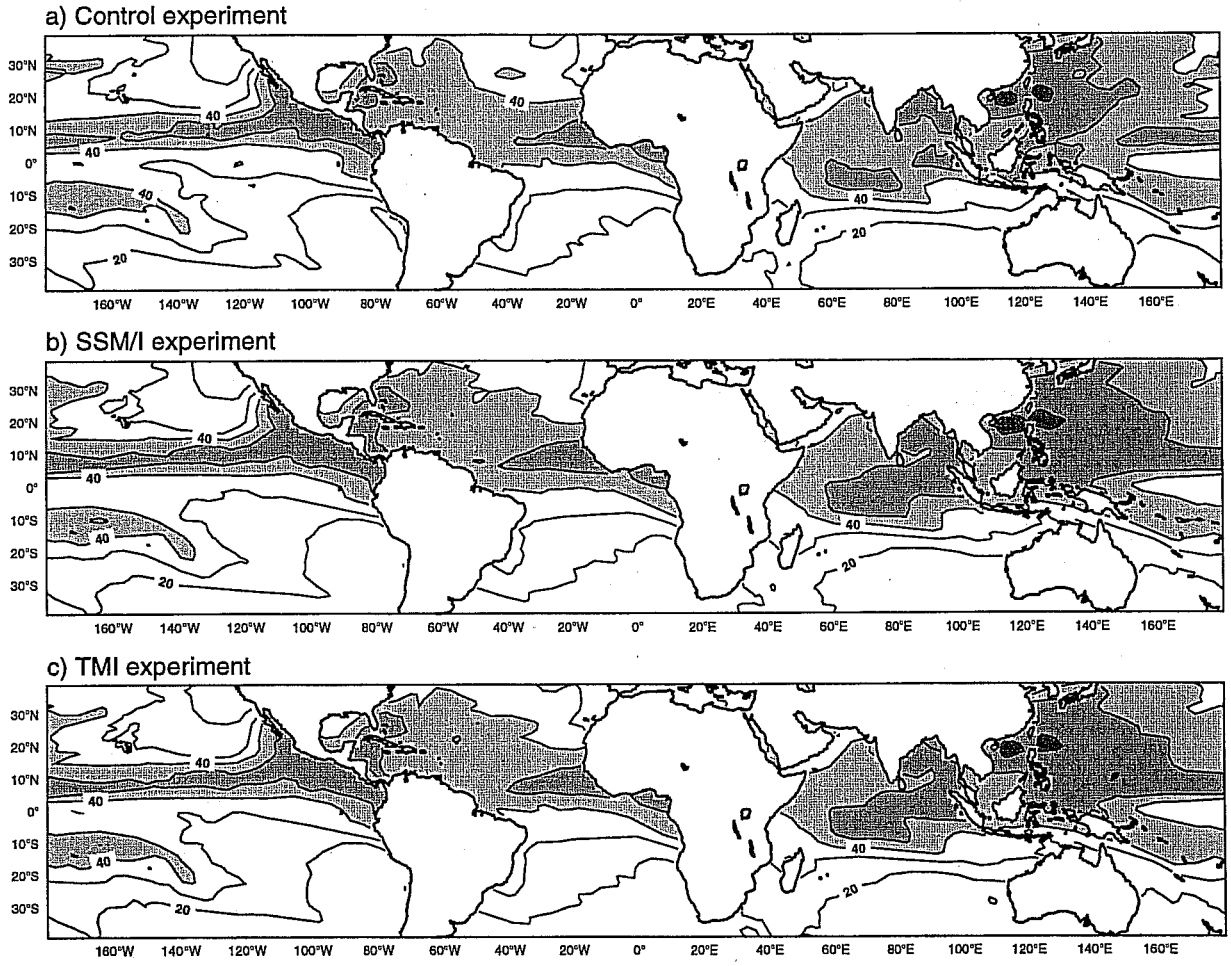

Figure 5: *Mean TCWV field from 4D-Var analyses averaged over the two-week period. (a) Control experiment, (b) SSM/I experiment and (c) TMI experiment. Contours are every 10 kg* m^{-2} *and grey shading starts at 40 kg* m^{-2}

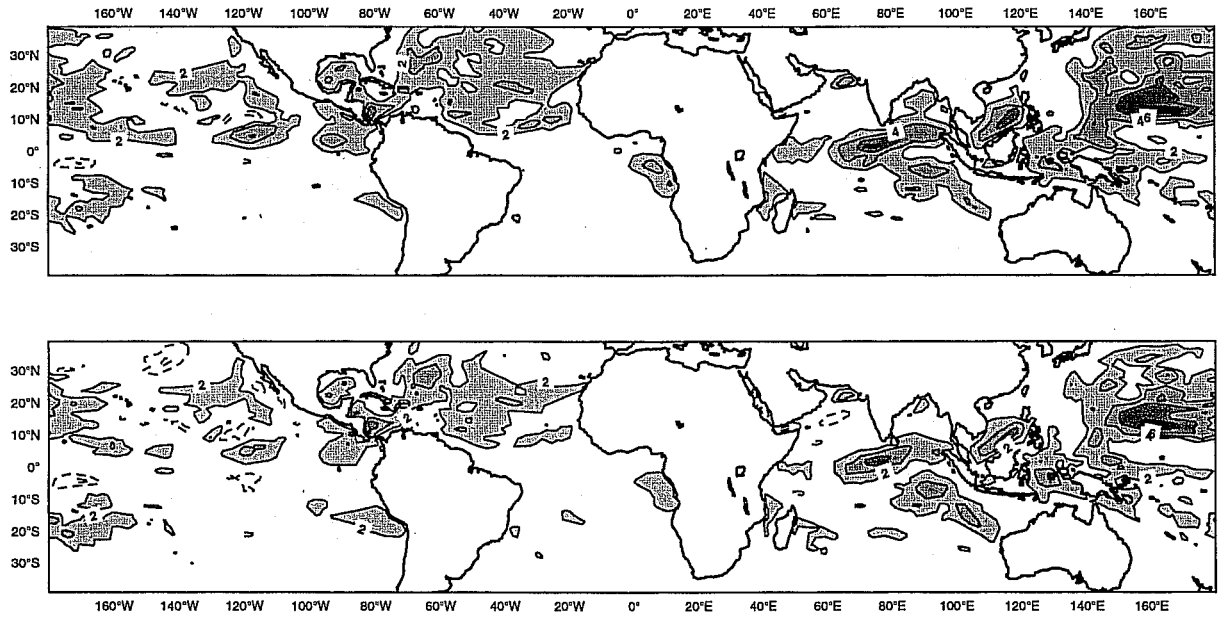

Figure 6: *Mean TCWV differences from 4D-Var analyses averaged over the two-week period. SSM/I experiment minus Control experiment (top panel) and TMI experiment minus Control experiment (bottom panel). Grey shading starts at 2 kg m^{-2}. Solid lines are for positive values, every 2 kg m^{-2} from 2 kg m^{-2}. Heavy dashed lines are for negative values, every -2 kg m^{-2} from -2 kg m^{-2}.*

The RMS of TCWV increments for the three experiments are shown in Fig. 7. For the Control experiment the values are generally small because of the scarcity of humidity observations over ocean, except near radiosonde launching places where they reach very large values up to 6.7 kg m^{-2}. For SSM/I and TMI experiments "1D-Var TCWV observations" are regularly assimilated in the tropical belt leading to a global increase of the RMS field compared to the Control experiment. Nevertheless, TMI experiment gives generally smaller RMS values than SSM/I ones, particularly in the Western Pacific and at radiosonde locations, showing that the assimilation of TMI brightness temperatures improves the quality of short-range forecasts of specific humidity.

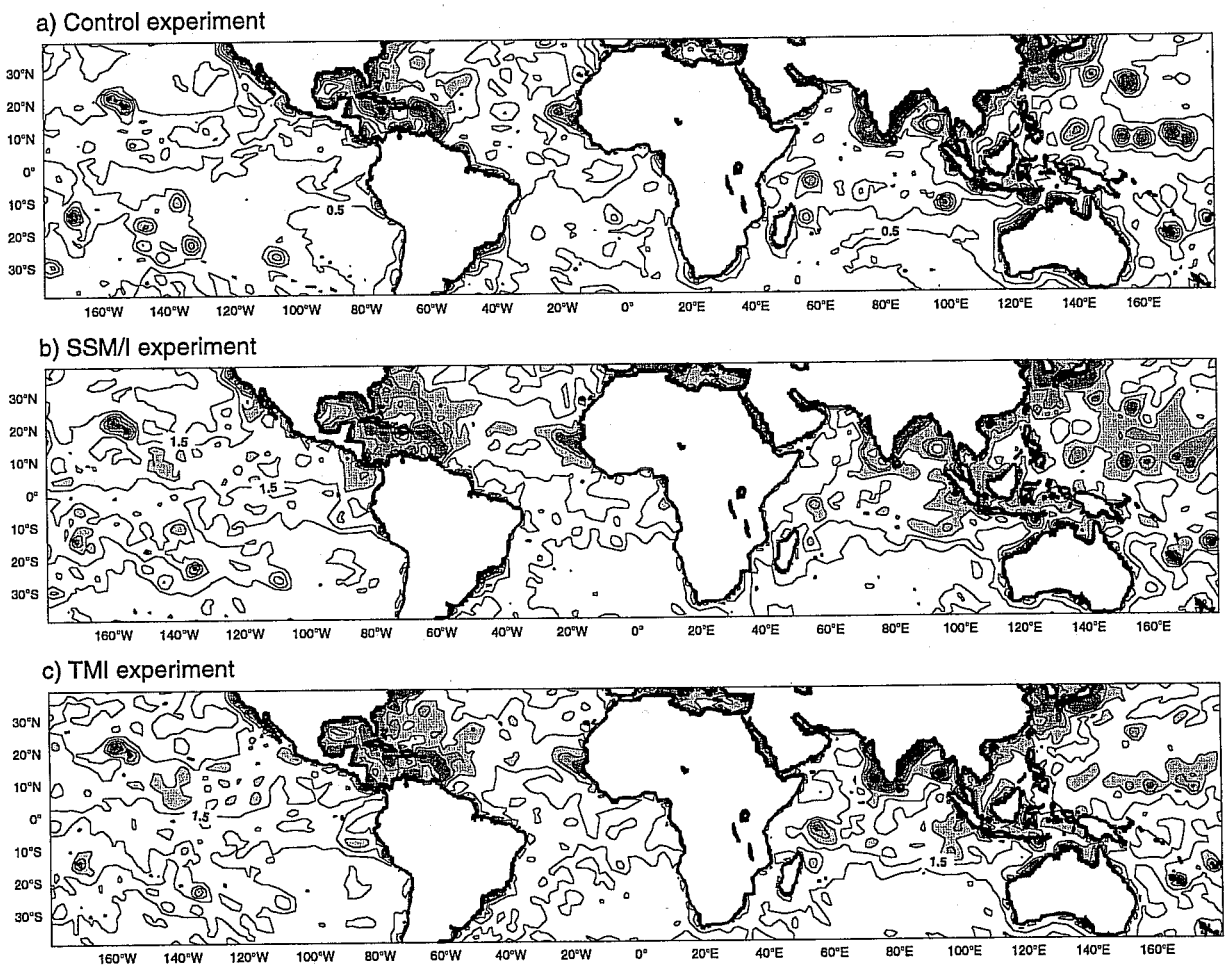

Figure 7: *Root mean square of TCWV increments in kg m^{-2} averaged over the two-week period. The increment field is obtained by computing analysed field minus background field (short-term forecast). (a) Control experiment, (b) SSM/I experiment and (c) TMI experiment. Contours are every 0.5 kg m^{-2} and grey shading starts at 2 kg m^{-2}.*

Experiment	Mean of analysed wind speed	RMS of wind speed increments
Control	6.208	0.654
SSM/I	6.213	0.643
TMI	6.277	0.640

Table 7: *Global values over ocean for the 10-m wind speed. Units are in* ms^{-1}

5.3 Analysis of sea surface wind speed

Results for the 10-m wind speed analysed by 4D-Var are given in Table 7. Global mean values for the three experiments show only small differences (around 1%). TMI experiment corresponds the highest value because its 1D-Var SSWS estimates provide on average stronger winds compared to the SSM/I estimates and to the model. Global mean values for RMS SSWS increments are very close for the three experiments with differences of around 2% (see Table 7). The use of SSM/I or TMI data tends to decrease the RMS and thus provides a slightly better 4D-Var analysis of low level winds.

The reason why very similar results are found for the Control, SSM/I and TMI analyses of the low level wind speed lies in the global observation coverage. Unlike the humidity analysis for which few data are assimilated, ERS-2 scatterometer and BUOY/SHIP observations over ocean are also used operationally in 4D-Var on top of SSM/I SSWS.

6 Impact on forecasts

6.1 Hydrological cycle

Changes in the humidity analysis have an impact on the short-range forecast of rainfall rate. This is illustrated in Fig. 8 which shows the global surface rainfall rate over oceans accumulated over the 12 past hours as a function of the forecast range. The curve corresponding to the Control experiment reflects mostly the model equilibrium since it makes use of very few humidity data in 4D-Var assimilation. Its "zigzag" shape is related to the diurnal cycle. Curves for SSM/I and TMI experiments start with large surface rainrates at the beginning of the forecasts and they rapidly decrease. This "spin-down" behavior is due to an imbalance of the hydrological cycle during the first days of the forecasts. TMI observations have a positive impact on the spin-down which is reduced compared to SSM/I experiment. This is because TMI observations provide a drier initial atmosphere compared to SSM/I ones leading to less precipitation at the beginning of the forecasts.

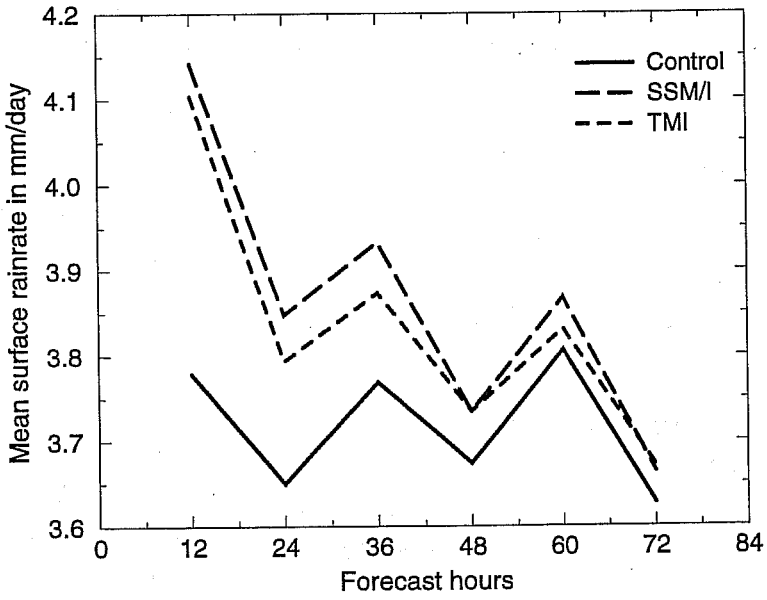

Figure 8: *Global average of surface rainfall rate over the two week period as a function of forecast range. The surface rainrate is here the accumulated surface rainrate between T-12 hours and T, T being the forecast hour.*

6.2 Objective scores

In this subsection results are given for the full globe. To assess the impact on the forecasts of assimilating 1D-Var products from SSM/I or TMI brightness temperatures, the anomaly correlation for the geopotential at 1000 hPa is computed up to day-6. Results for the Northern (between +90° and +20° latitude) and the Southern (between -20° and -90° latitude) hemispheres are shown in figure 9. For the Northern hemisphere TMI experiment provides slightly better scores than the other two experiments. This improvement is significant to the 5% level in the medium range. In the Southern hemisphere, TMI experiment improves less the performances than SSM/I one with a 5% level significance in the medium range. This can be explained by two reasons. Firstly, very few humidity data are available in the Southern hemisphere apart from SSM/I or TMI observations. Secondly, less TMI observations are used compared to SSM/I because of the TRMM coverage (tropics and sub-tropics only).

Tropical wind scores at 1000 hPa and 200 hPa up to day-4 are displayed on Fig. 10 in terms of RMS errors. They are computed against their own analysis, as the tropical analyses in the three experiments are significantly different from the operational ones. For low level winds, a reduction of the RMS error is found for TMI and SSM/I experiments compared to the Control. Nevertheless, TMI shows less improvement than SSM/I in the medium range (significant to the 5% level). This is likely to come from problems previously mentioned: a rather poor representativeness of TMI SSWS with respect to the model wind and the assumption of a constant zenith angle in the radiative transfer model. At 200 hPa, the best scores are found for

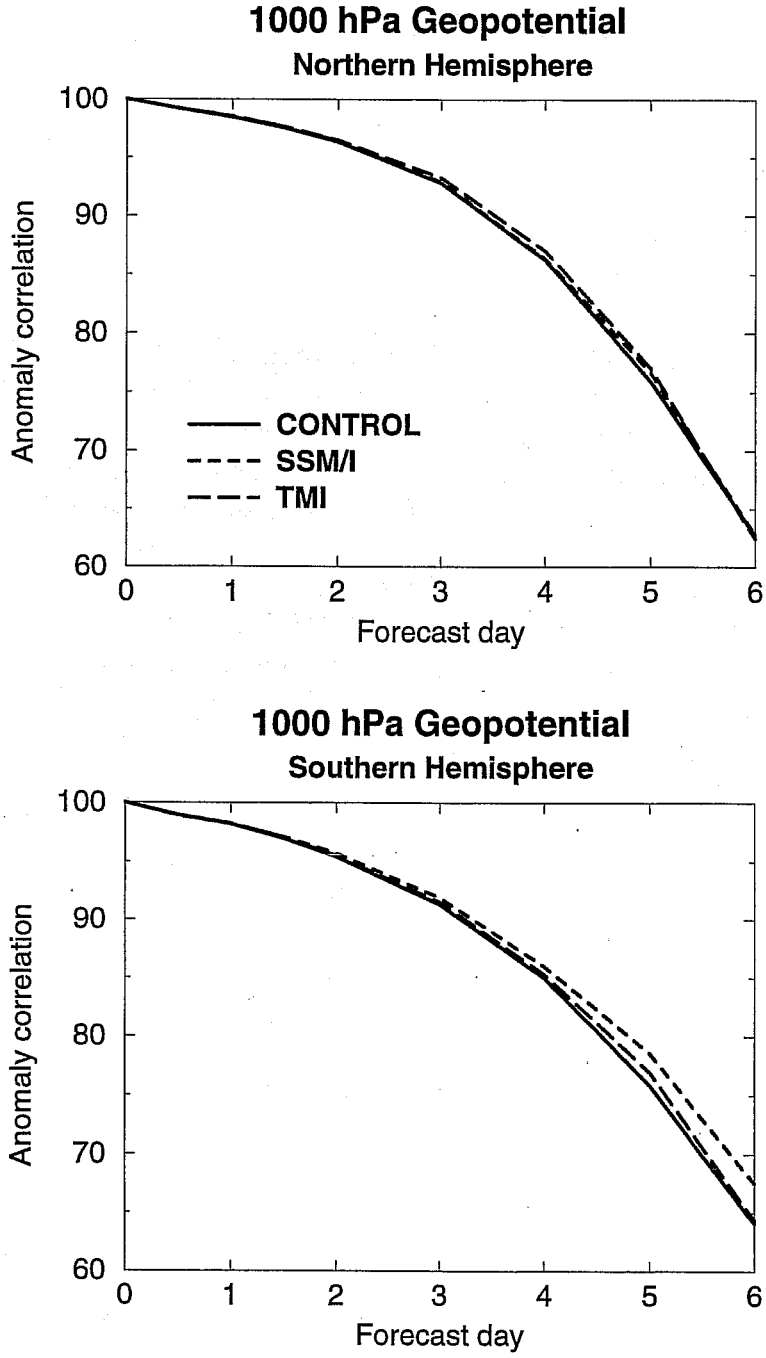

Figure 9: *Anomaly correlation of the geopotential at 1000 hPa averaged over 15 forecasts (7 to 21 September 1999) issued from 4D-Var. The top panel is for the Northern hemisphere and the bottom panel is for the Southern hemisphere. Control experiment corresponds to the solid line, SSM/I experiment to the dashed line and TMI experiment to the dotted line.*

TMI experiment while SSM/I experiment show a deterioration compared to TMI and Control experiments that is significant at the 5% level in the short range. This effect is probably related to the latent heat release produced by the initial too moist atmosphere in the SSM/I experiment that modifies the upper tropospheric divergent circulation.

7 Conclusions

In this paper, the impact of assimilating TMI brightness temperatures instead of SSM/I ones in the operational ECMWF 4D-Var system was investigated. SSM/I brightness temperatures are used operationally at ECMWF through a one-dimensional variational approach. The 1D-Var method is used to retrieve simultaneously profiles of specific humidity, SSWS and LWP. SSWS and TCWV (derived from specific humidity profiles) are then assimilated in the operational ECMWF 4D-Var analysis system. Since November 1997, TMI radiances are also available. TMI is the microwave radiometer on board TRMM which samples the tropics and the sub-tropics. Its characteristics are slightly different from SSM/I: two additional channels at 10.65 GHz vertical and horizontal polarization and a water vapour channel at 21.3 GHz instead of 22.235 GHz. A constant zenith angle is used in the radiative transfer model for the simulation of TMI brightness temperatures. Simulations using a large variety of atmospheric conditions have shown that this assumption has a small impact on the estimation of brightness temperatures (bias < 0.5 K).

Theoretical accuracies of 1D-Var retrievals were computed. Results show that TMI data provide in theory more accurate 1D-Var SSWS and TWCV products than SSM/I ones. The reason is that TMI observations contain more information on surface and atmospheric parameters than SSM/I observations by the different choice of frequencies. Nevertheless, these accuracy calculations do not take into account the assumption of a constant zenith angle in the radiative transfer model. This means that the accuracy for TMI SSWS should be smaller than its theoretical estimation.

Three 4D-Var assimilation experiments were run for a two-week period. SSM/I experiment is the operational configuration that makes use of SSM/I TCWV and SSWS. Control experiment is identical but without SSM/I TCWV and SSWS. TMI experiment is identical to SSM/I one except that it makes use of TMI SSWS and TCWV instead of SSM/I SSWS and TCWV.

Statistics of model departures from obervations show that for both SSM/I and TMI experiments, part of the information from TCWV and SSWS 1D-Var estimates is used in 4D-Var analysis. The positive bias of the background departure (observation minus background) for SSWS with TMI is likely to be related to a representativeness problem: each TMI SSWS estimate is representative of a much smaller area than the model grid box. This problem is negligible for TCWV because the TCWV field is homogeneous at the scale of a model grid box.

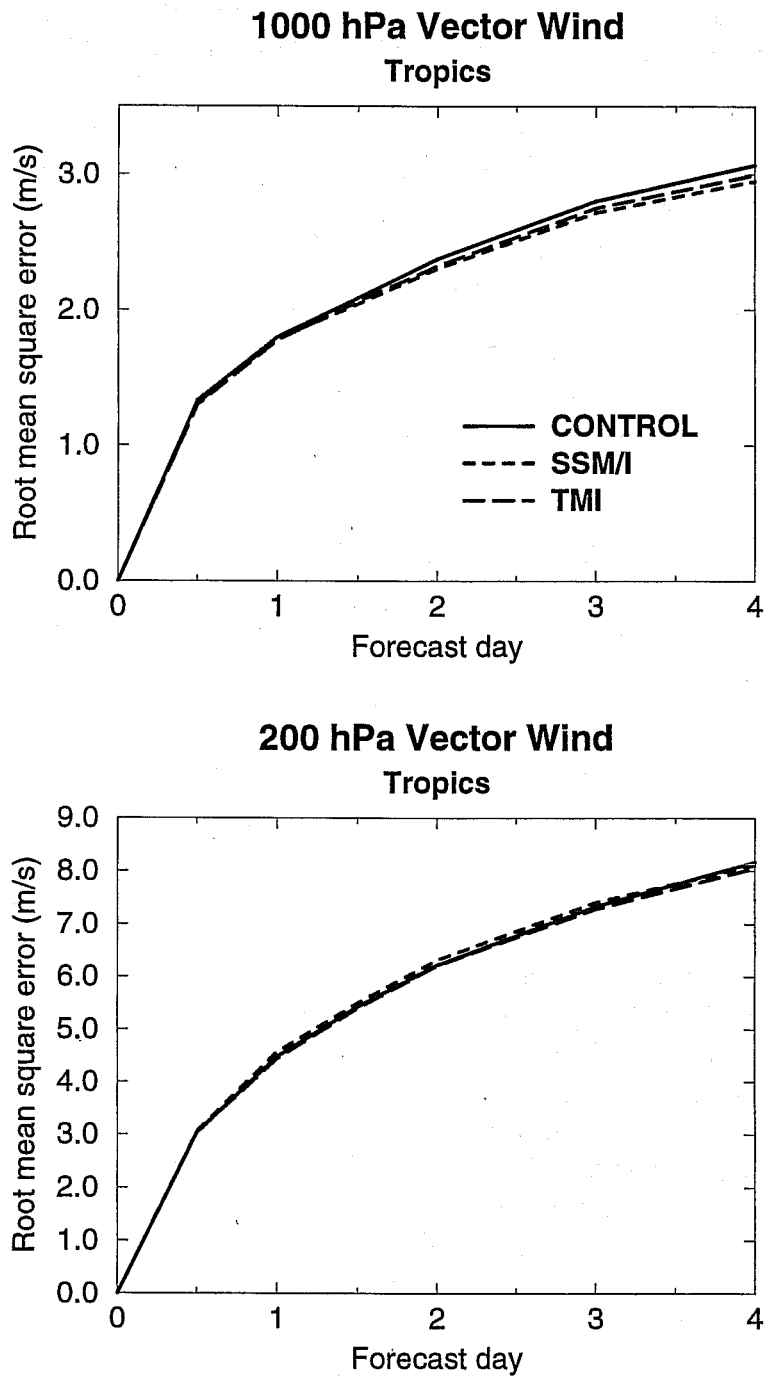

Figure 10: *Root mean square error scores for tropical winds verified against its own analysis at 1000 hPa (top panel) and 200 hPa (bottom panel) averaged over 11 forecasts from 4D-Var assimilation. Control experiment corresponds to the solid line, SSM/I experiment to the dashed line and TMI experiment to the dotted line.*

Since very few humidity data are available over ocean, both SSM/I or TMI observations provide a large piece of information to the 4D-Var system for humidity analysis. There is a very good consistency between SSM/I and TMI TCWV analysed fields in the latitude band covered by TMI sampling. TMI observations tend to increase slightly less the global humidity. The impact on humidity analysis is more positive when using TMI data than SSM/I ones as shown by the reduction of the RMS TCWV increments. The impact of both SSM/I and TMI observations on the low level wind analysis is positive but small because other types of wind data are also assimilated over ocean.

The consequence on the forecasts is a reduction of the precipitation spin-down at the beginning of the forecast when TMI TCWVs are used instead of SSM/I ones. Global forecast scores for TMI experiment are all better than the Control experiment. Performances of SSM/I experiment are improved compared to the other two experiments for the Southern hemisphere and for the tropical low level winds. But SSM/I scores are worse than TMI ones for the Northern hemisphere and for the tropical wind at 200 hPa.

All these results shows that the TMI characteristics, and in particular the availability of the 10 GHz channels, allow an improvement of the humidity analyses in the Tropics with respect to the operational configuration which makes use of SSM/I data. However, TMI brightness temperatures are likely not to be assimilated operationally at ECMWF because of the short life time of the research satellite TRMM (three years).

Acknowledgements

TRMM is a joint NASA/NASDA mission (spacecraft launched in November 1997). We acknowledge NASA and NASDA for opening the TRMM data to Euro TRMM, a consortium of scientists from Centre d'étude des Environnements Terrestre et Planétaires (France), German Aerospace Research Establishment (Germany), Istituto di Fisica dell Atmosfera (Italy), Max Planck Institute für Meteorologie (Germany), Rutherford and Appleton Laboratory (U. K.), University of Essex (U.K.), Université Catholique de Louvain (Belgium), University of Munich (Germany) and European Centre for Medium-Range Weather Forecasts (U.K.). Euro TRMM is funded by European Commision and European Space Agency and is coordinated by Pedro Poires Baptista (ESA/ESTEC) and Jacques Testud (CNRS/CETP).

References

Alishouse, J.C., Snyder, S.A., Vongsathorn, J., and Ferraro, R.R., 1990: Determination of oceanic total precipitable water from the SSM/I. *IEEE Trans. Geosci. Remote Sensing*, **28**, 811–816

Bauer, P. and Schluessel, P., 1993: Rainfall, total water, ice water and water vapour over sea from polarized microwave simulations and specical sensor microwave/imager data. *J. Geophys. Res.*, **98**, 20737–20759

Courtier, P., Thépaut, J.-N. and Hollingsworth, A., 1994: A strategy for operational implementation of 4D-Var using an incremental approach. *Q. J. R.. Meteorol. Soc.*, **120**, 1367–1387

Ferraro, R.R., Weng, F., Grody, N.C. and Basist, A., 1996: An eight-year (1987-1994) time series of rainfall, clouds, water vapor, snow cover, and sea ice derived from SSM/I measurements. *Bull. Amer. Meterol. Soc.*, **77(5)**, 891–905

Gérard, É. and Eymard, L., 1998: Remote sensing of integrated cloud liquid water: development of algorithms and quality control. *Radio Science*, **33**, 433–447

Gérard, É. and Saunders, R.W., 1999: 4D-Var assimilation of SSM/I total column water vapour in the ECMWF model. *Q. J. R. Meteorol. Soc.*, **125**, 3077–3101

Gérard, É. and McNally, T., 1999: Assimilation of SSM/I 1D-Var 10 metre wind speed. *ECMWF internal document* RD Memo R43/EG/73

Goodberlet, M.A., Swift, C.T., and Wilkerson, J.C., 1990: Ocean surface wind speed measurements of the special sensor microwave /imager (SSM/I). *IEEE Trans. Geosci. Remote Sensing*, **28**, 823–827

Hollinger, J.P., Peirce, J.L., and Poe, G.A., 1990: SSM/I instrument evaluation. *IEEE Trans. Geosci. Remote Sensing*, **28**, 781–789

Karstens, U., Simmer, C., and Ruprecht, E., 1994: Remote sensing of cloud liquid water. *Meteorol. Atmos. Phys.*, **54**, 157–171

Klinker, E., Rabier, F., Kelly, G., and Mahfouf, J.-F., 2000: The ECMWF operational implementation of four-dimensional variational assimilation. III: Experimental results and diagnostics with operational configuration. *Q. J. R. Meteorol. Soc.*, **126**, 1191–1216

Kummerow, C., Olson, W., and Giglio, L., 1996: A simplified scheme for obtaining precipitation and vertical hydrometeor profiles from passive microwave sensors. *IEEE Trans. Geosci. Remote Sensing*, **34**, 1213-1232

Kummerow, C., Barnes, W., Kozu, T., Shiue, J., and Simpson, J., 1998: The Tropical Rainfall Measuring Mission (TRMM) sensor package. *J. Atmos. Ocean. Technol.*, **15**, 809–817

Mahfouf, J.-F., 1999: Influence of physical processes on the tangent-linear approximation. *Tellus*, **51A**, 147–166

Mahfouf, J.-F., and Rabier, R., 2000: The ECMWF operational implementation of four-dimensional variational assimilation. II: Experimental results with improved physics. *Q. J. R. Meteorol. Soc.*, **126**, 1171–1190

Phalippou, L., 1996: Variational retrieval of humidity profile, wind speed and cloud liquid water path with the SSM/I: Potential for numerical weather prediction. *Q. J. R. Meteorol. Soc.*, **122**, 327–355

Phalippou, L., and Gérard, É., 1996: Use of precise microwave imagery in numerical weather prediction. *Study report to the European Space Agency*, 70 pp. (available from ECMWF)

Rabier, F., Järvinen, H., Klinker, E., Mahfouf, J.-F., and Simmons, A., 2000: The ECMWF operational implementation of four-dimensional variational assimilation. I: Experimental results with simplified physics. *Q. J. R. Meteorol. Soc.*, **126**, 1143–1170

Rodgers, C.D., 1976: Retrieval of atmospheric temperature and composition from remote sensing of thermal radiation. *Rev. Geophys. Space Phys.* **14**, 609–624

Simpson, J., Kummerow, C., Tao, W.-K., and Alder, R.F., 1996: On the Tropical Rainfall Measuring Mission (TRMM). *Meteor. Atmos. Phys.*, **60**, 19–36

Stoffelen, A., and Anderson, D., 1994: The ECMWF contribution to the characterisation, interpretation, calibration and validation of ERS1 scatterometer backscatter measurements and winds, and their use in numerical weather prediction models. *Final Report, ESA contract 9097/90/NL/BI*, (available from ECMWF)